IV Journeys in Multiphase Flows (JEM2017)
March 27-31, 2017 - São Paulo, Brazil

PaperID: JEM-2017-0049

DYNAMIC ANALYSES OF SPREADING DROPLETS ON NANOPARTICLES-COATED ALUMINUM PLATES

Erivelto dos Santos Filho
erivelto.usp@gmail.com
Debora Carneiro Moreira
dcmoreira@id.uff.br
Gherhardt Ribatski
ribatski@sc.usp.br
Heat Transfer Research Group – Department of Mechanical Engineering – São Carlos Engineering School, University of São Paulo (EESC/USP) – Av. Trabalhador São-Carlense, 400, Parque Arnold Schimidt, São Carlos, SP, Brazil.

Abstract. *Phase-change heat transfer is significantly influenced by surfaces' wettability, which has turned this into one of the hottest investigated topics in multiphase field. The objective of the present work is to evaluate the dynamic wettability of neat and alumina-coated aluminum plates. The alumina-coated plate was produced through pool boiling of 300 ml of a water-based nanofluid containing 0.1% in volume of 20–30 nm* γ*-*Al_2O_3 *nanoparticles over an as-received aluminum plate. The wettability of both neat and alumina-coated plates was assessed by side-on and top-down methods, using a high-speed camera to acquire images of 8* μl *deionized water droplets spreading on these surfaces. The contact line displacement and velocity were evaluated using both methods and the time-variation of contact angle was assessed by the side-on method. Good agreement and repeatability among the tests were observed. The deposition of nanoparticles on the aluminum plate resulted in a superwetting surface, and it could be noted that the spreading mechanism changed from inertially-driven to capillarity-driven on such surface.*

Keywords: *Super-wetting, Hydrophilic, Wettability, Contact angle, Nanofluid.*

Topic of interest: *Particle, bubble and drop dynamics*

1. INTRODUCTION

Heat transfer between solids and fluids is a subject of major concern for science and technology, since the search for highly efficient industrial processes and equipments' development is usually related to improved heat transfer. During the last years, advances in micro- and nano-fabrication techniques have enabled various investigations concerning heat transfer in micro- and nanostructured surfaces, which showed an overall augmentation of single or multi-phase heat transfer coefficients, among other parameters. In a recent review article, Kandlikar (2016) pointed out that the potential for boiling heat transfer in microchannels is yet to be achieved, and that the most promising way to do so is through optimized designs for each desired application, including micro- and nanostructures on microchannels. Micro- and nanostructured surfaces were also highlighted as promising solutions to enhance pool and flow boiling heat transfer in an extensive review carried out by Shojaeian and Kosar (2015). Betz *et al.* (2013) have fabricated surfaces containing hexagonal micropillars with alternating wettability and measured the density of active nucleation sites on pool boiling experiments. They concluded that these surfaces with juxtaposed wettabilities have better performance than surfaces with uniform wettability because of wetting lines movements and capillarity phenomena. Jo *et al.* (2012) conducted an experimental study on pool boiling heat transfer on identical surfaces with distinct wettabilities and examined the effect of this parameter on heat transfer coefficient and critical heat flux (CHF). In this work, they suggested that both surface wettability and capillary wicking effects contribute to improve CHF and heat transfer coefficient. In another work, Jo *et al.* (2015) also studied nucleate boiling heat transfer on surfaces with designed heterogeneous wettabilities. A hydrophilic monolayer acted to separate vapor and liquid paths, and improvements in boiling heat transfer were observed, especially higher CHF. The influence of surface texturing in critical heat flux was also investigated by Dhillon *et al.* (2015), and they noted the existence of a maxima in CHF enhancement. They investigated the dynamics of dry spot heating and rewetting phenomena, relating the CHF enhancement to rewetting of a hot dry spot on the boiling surface. Yang *et al.* (2016) used the plasma immersion ion implantation method to produce black silicon surfaces and investigated the wettability and boiling heat transfer performances of the fabricated surfaces. Both the active nucleation sites and the contact angle were increased in black silicon surfaces.

According to many recent studies, among numerous parameters that may influence in solid-fluid heat transfer (Betz *et al.*, 2013; Jo *et al.*, 2015; Dhillon *et al.*, 2015; Yang *et al.*, 2016; Villa *et al.*, 2016), surface wettability seems to strongly affect such behavior and can be readily tuned with micro- and nano-structuring. However, nano-manufacturing techniques are often expensive and hardly up-scalable, which are limiting factors for industrial applications that often require low-cost and macro-scale solutions. In addition, most of the times these techniques cannot be applied in curved surfaces or in operational equipment. In this sense, this work comprises a dynamic wettability evaluation of neat and nanoparticles-coated aluminum plates. The nanostructured surface was produced by nanofluid pool boiling process, which is a facile fabrication method. Wettability analyses of both surfaces were carried out using side-on and top-down methods and a high-speed camera to record images of deionized (DI) water droplets spreading on these surfaces at 3500 and 1000 fps, respectively. The contact line velocity was measured using both methods with good agreement between the datasets obtained for each sample, while the dynamic contact angle was measured only through the side-on method. Good repeatability of the tests was also noticed. Results show that superwetting surfaces were obtained with the deposition of nanoparticles through pool boiling of alumina-water nanofluid, in which a change from inertial to capillarity-driven spreading mechanisms could also be noted.

2. MATERIALS AND METHODS

2.1 Samples fabrication

Two aluminum plates with 10 cm $\times$ 10 cm $\times$ 0.2 cm and with an average roughness equal to 570 nm were used to produce the samples. The nanoparticles-coated sample was produced through a pool-boiling process of a water-based nanofluid containing 0.1% in volume of nearly spherical Al_2O_3 nanoparticles fabricated by NanoAmor, with diameters ranging from 20 to 30 nm. First the nanofluid was fabricated using 300 ml of deionized water and the amount of nanoparticles corresponding to the desired volume fraction of the nanofluid. The resulting blend was sonicated during 30 minutes, then the nanofluid was transferred to the boiling apparatus depicted in Fig. 1 and the boiling process was carried out for 45 minutes.

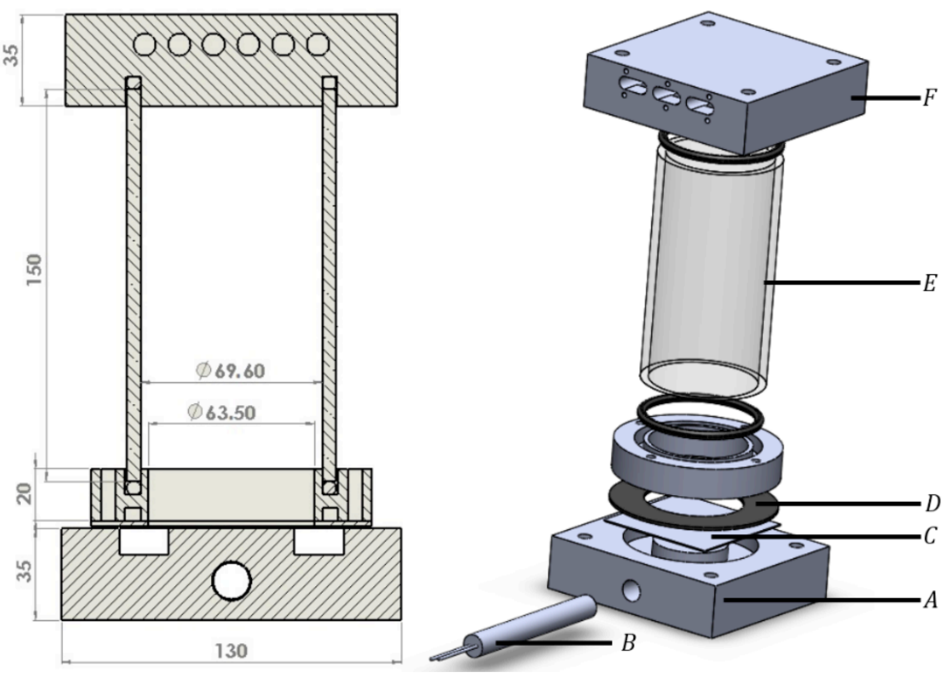

Figure 1. Boiling apparatus (dimensions in mm).

This apparatus consists of a bottom aluminum base (A) heated by a cartridge heater (B) of 245W, an aluminum plate (C), which is the sample where the deposition occurs, a rubber disk (D) to seal all the bottom part, a borosilicate glass tube (E), and the cooling aluminum block (F) to condense the water vapor, maintaining the same amount of water in the system. A thermal bath connected into a water loop allows the cooling of the aluminum block (F) through machined channels.

2.2 Wettability analyses

The wettability evaluation method was based on the analysis of images obtained from a DI-water droplet spreading through the neat and nanoparticles-coated horizontal flat surfaces. An Eppendorf Research Plus micropipette was used to deposit the droplets on the surfaces, providing an error of 0.8%, and a high speed camera (CamRecord 600) with lens AF MICRO NIKKOR 60 mm was employed to acquire the images. For the top-down measurements, the camera was set to record images for 1s at 1000 frames per second (fps) with resolution of 1280×512 pixels, while for the side-on method it was set to acquire images at 3500 fps for 1s, with resolution of 1280×128 pixels. To ensure that the sample's surface was perpendicular to the camera, a digital inclinometer (DNM 60L Professional) with resolution of 0.1° was used. The droplet was released with a small hand perturbation on the opposite side of the pipette. In order place the DI-water droplet in similar conditions on all surfaces, the distance between the surface and the needle tip was kept at 15 mm. To verify the homogeneity of the sample covered by nanoparticles and also repeatability of the tests, three tests were carried out with each sample for both methods separately. The obtained images that reveal the side-on or top-down wetted areas by the DI-water were analyzed through the software ImageJ V. 1.49, which is a Java-based software developed at the National Institutes of Health (https://imagej.nih.gov/ij/), then the contact line displacement, the contact line velocity, and contact angle variations were evaluated.

3. RESULTS

Results of spreading droplets are shown below. Fig. 2(a) reveals the variation of the radii of droplets spreading on the neat aluminum plate and on the surfaces coated with nanoparticles, while Fig. 2(b) presents the absolute difference of measured radii with both methods. Each curve represents the average of three tests, and a maximum dispersion of 9% was observed. Images were acquired using the side-on (Frontal) and the top-down (Top) methods, and a good agreement can be observed between the obtained results for each sample, with average and maximum deviations for the neat sample equal to 1.3% and 7.2%, and 5.0% and 10.7% for the Al_2O_3-coated sample.

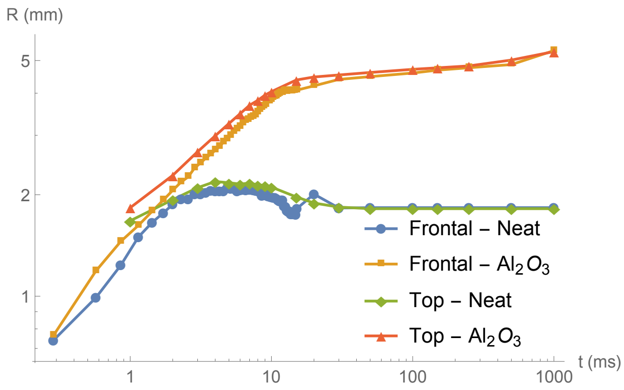

(a)

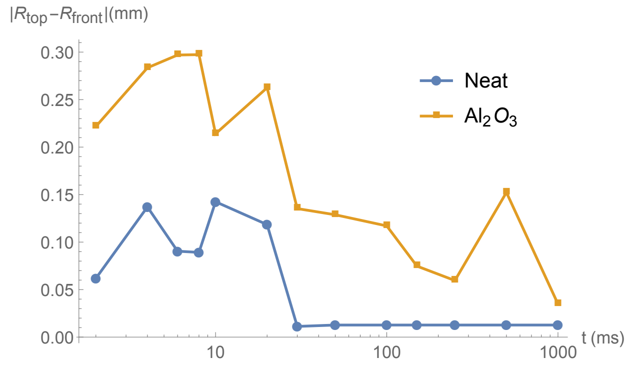

(b)

Figure 2. Time variation of droplets' radii on neat and nanoparticles-coated surfaces evaluated through side-on (Frontal) and top-down (Top) methods (a), and absolute difference between both methods.

According to Fig. 2(a) the deposition of nanoparticles on the aluminum plate resulted in a super-wetting surface, where the droplet spreads not only for the first milliseconds, but continues to spread due to capillarity effects through the porous nanoparticles layer. One can also observe that the radii of the droplets deposited on the Al_2O_3-coated sample after 1 s have risen by 2.5 times, if compared to the droplets on the neat surface, even though the amount of liquid was the same in each test, which corroborates the influence of the nanoparticles-layer on wettability and capillarity of the surface. In addition, it could be noticed that the spreading droplets only follow the power-law during the first milliseconds, when it is driven by inertia and wettability, then the spreading mechanism change to capillarity-driven and the behavior is modified.

The contact line velocity was calculated based on the displacement of the contact lines and the time intervals between consecutive images. Figure 3 shows the time variation of contact line velocities assessed by top-down and side-on methods on both surfaces. Only the values calculated for the first 30 milliseconds are displayed in this figure because from this time on the spreading velocities are negligible.

It is clear in the data presented in Fig. 3 that contact line velocities of droplets deposited on the neat surface quickly goes to values close to zero, and the observed oscillations are due to changes in the dynamic contact angle that occur before the droplet turns static. The same oscillations can be observed on droplets spreading over the surfaces containing nanoparticles, but the velocities are generally greater than zero, because the droplets are still spreading. It can be seen that this phenomenon was only captured at the higher acquisition rate that was employed only for side-on measurements due to a small resolution in one direction, which would hinder the acquisition of the whole wetted areas on top-down tests. Once again, a good agreement was obtained between side-on and top-down methods. Finally, variations of contact angle were also evaluated and are presented in Fig. 4.

Figure 4 shows some oscillation of the contact angle during the first milliseconds, especially on the neat surface, because the maximum diameter of the droplet is quickly achieved and the remaining energy is dissipated through droplet's movements, which only act in sense of changing the contact angle, since the contact line is static. On the other hand, less oscillations are observed on the Al_2O_3-coated sample, since the droplet continues to spread. It is interesting to point

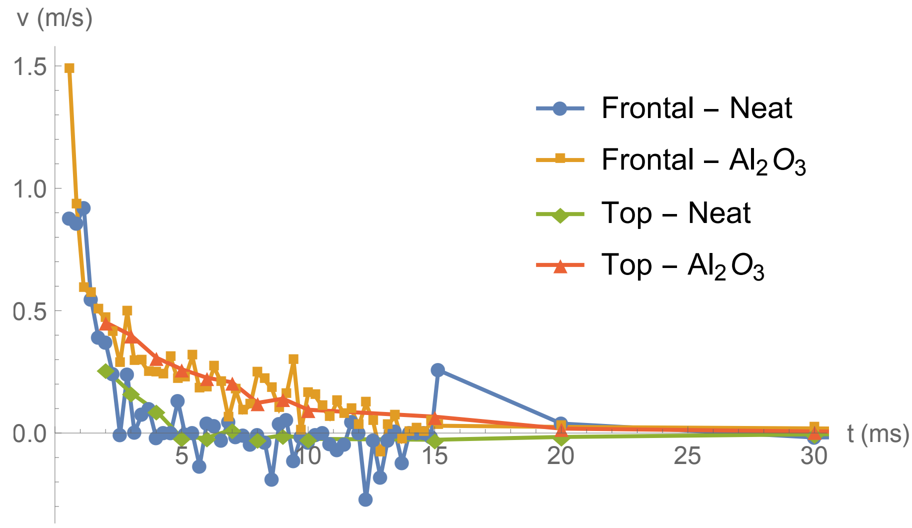

Figure 3. Time variation of contact line velocities on neat and nanoparticles-coated surfaces evaluated through side-on (Frontal) and top-down (Top) methods.

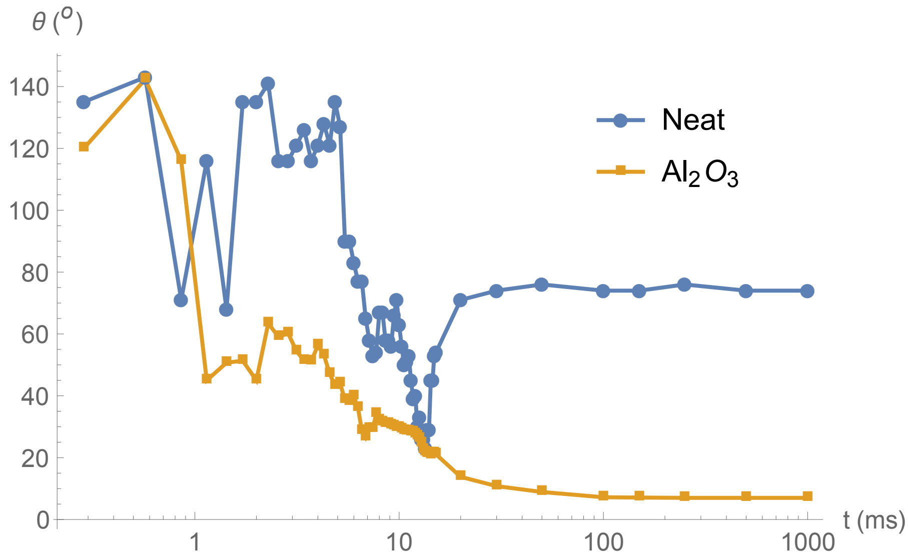

Figure 4. Time variation of contact angle on neat and nanoparticles-coated surfaces evaluated through side-on (Frontal) method.

out that after approximately 30 ms the contact angle was almost static for both sample, even though the droplet is still spreading through the coated surface. As a final comment, one should notice that the deposition of Al_2O_3 nanoparticles on the aluminum plates resulted in significant increase in wettability, as can be concluded by the change in contact angle from 74° on the neat sample to 7° on the coated sample.

4. CONCLUSIONS

This work presented dynamic wettability evaluations of neat and nanoparticles-coated aluminum plates. The deposition of nanoparticles on the aluminum plate was carried out by pool boiling of a nanofluid containing 0.1% of 20–30 nm Al_2O_3 nanoparticles. Both side-on and top-down methods were employed in wettability analyses, such that the contact line displacement of DI-water droplets could be assessed and the contact line velocities calculated. Images were recorded at 3500 and 1000 fps for side-on and top-down methods, respectively. Results show that a superwetting surface was obtained with the deposition of nanoparticles through pool boiling of alumina-water nanofluid, in which a change from inertial to capillarity-driven spreading mechanisms was noticed. A good agreement was observed between the datasets obtained through the distinct methods (side-on and top-down). Although the droplet was still spreading through the nanoparticles-covered plate after 1 s, measured contact angles achieved static values after 30 ms for both samples. Nevertheless, the highest acquisition rate enabled the observation of advancing and receding effects while the droplets were spreading.

5. ACKNOWLEDGEMENTS

The authors gratefully acknowledge the financial support provided by NANOBIOTEC-CAPES, and CNPq (150389/2016-7). The technical support given to this investigation by Hélio Donisetti Trebi is also appreciated and deeply recognized.

6. REFERENCES

Betz, A.R., Jenkins, J., Kim, C.J. and Attinger, D., 2013. "Boiling heat transfer on superhydrophilic, superhydrophobic, and superbiphilic surfaces". *International Journal of Heat and Mass Transfer*, Vol. 57, pp. 733–741.

Dhillon, N.S., Buongiorno, J. and Varanasi, K.K., 2015. "Critical heat flux maxima during boiling crisis on textured surfaces". *Nature Communications*, Vol. 6, p. 8247.

Jo, H., Kim, S., Kim, H., Kim, J. and Kim, M.H., 2012. "Nucleate boiling performance on nano/microstructures with different wetting surfaces". *Nanoscale Research Letters*, Vol. 7, pp. 242–250.

Jo, H., Yu, D.I., Noh, H., Park, H.S. and Kim, M.H., 2015. "Boiling on spatially controlled heterogeneous surfaces: Wettability patterns on microstructures". *Applied Physics Letters*, Vol. 106, p. 181602.

Kandlikar, S.G., 2016. "Mechanistic considerations for enhancing flow boiling heat transfer in microchannels". *Journal of Heat Transfer*, Vol. 138, pp. 021504–2.

Shojaeian, M. and Kosar, A., 2015. "Pool boiling and flow boiling on micro- and nanostructured surfaces". *Experimental Thermal and Fluid Science*, Vol. 63, pp. 45–73.

Villa, F., Georgoulas, A., Marengo, M., Marco, P.D. and Coninck, J.D., 2016. "Pool boiling versus surface wettability characteristics". In *Proceedings of the World Congress on Momentum, Heat and Mass Transfer*.

Yang, L.X., Chao, Y.M., Jia, L. and Li, C.B., 2016. "Wettability and boiling heat transfer study of black silicon surface produced using the plasma immersion ion implantation method". *Applied Thermal Engineering*, Vol. 99, pp. 253–261.

7. RESPONSIBILITY NOTICE

The authors are the only responsible for the printed material included in this paper.